

# Mixing Natural and Synthetic Images for Robust Self-Supervised Representations

Reza Akbarian Bafghi<sup>\*1</sup> Nidhin Harilal<sup>\*1</sup> Claire Monteleoni<sup>1,2</sup> Maziar Raissi<sup>3</sup>

## Abstract

This paper introduces *DiffMix*, a new self-supervised learning (SSL) pre-training framework that combines real and synthetic images. Unlike traditional SSL methods that predominantly use real images, DiffMix uses a variant of Stable Diffusion to replace an augmented instance of a real image, facilitating the learning of cross real-synthetic image representations. The key insight is that while SSL methods trained solely on synthetic images underperform compared to those trained on real images, a blended training approach using both real and synthetic images leads to more robust and adaptable representations. Experiments demonstrate that DiffMix enhances the SSL methods SimCLR, BarlowTwins, and DINO, across various robustness datasets and domain transfer tasks. DiffMix boosts SimCLR’s accuracy on ImageNet-1K by 4.56%. These results challenge the notion that high-quality real images are crucial for SSL pre-training by showing that lower quality synthetic images can also produce strong representations. DiffMix also reduces the need for image augmentations in SSL, offering new optimization strategies.

## 1. Introduction

There has been a growing interest in using synthetic images for supervision (Sariyildiz et al., 2022; He et al., 2022b;a; Tian et al., 2023). These methods involve creating artificial images using generative models like GANs (Goodfellow et al., 2014) and Diffusion models (Ho et al., 2020), providing a vast and flexible data source. The appeal of synthetic image datasets lies in their ease of generation, wider range of semantic content, and minimal human intervention,

<sup>\*</sup>Equal contribution <sup>1</sup>Department of Computer Science, University of Colorado, Boulder, USA <sup>2</sup>INRIA, Paris, FR <sup>3</sup>Department of Mathematics, University of California, Riverside. Correspondence to: Reza Akbarian Bafghi <reza.akbarianbafghi@colorado.edu>, Nidhin Harilal <nidhin.harilal@colorado.edu>.

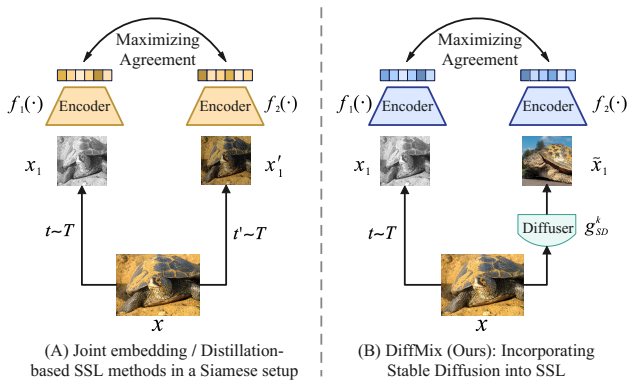


Figure 1. Comparison of our proposed DiffMix pipeline against existing Joint embedding/Distillation-based SSL methods that use a Siamese setting. DiffMix modifies a branch of augmentations to replace real image  $x'_1$  with a synthetically generated image  $\tilde{x}_1$

addressing key concerns in computer vision like cost efficiency and fairness in data collection and annotation. Although generative models address the issue of data scarcity, exclusive reliance on synthetic images for supervision is not without drawbacks. The main challenge has been the domain gap between synthetic and real-world data. Models trained only on synthetic images often struggle to adapt to real-world settings due to their limited exposure to the variability and complexity of natural images (Tremblay et al., 2018). This issue is particularly pronounced in large-scale image recognition tasks, where models trained on synthetic data typically underperform those trained on real images (Vanherle et al., 2022; Jeelani et al., 2023). In response to this, our research proposes a novel training framework that integrates both real and synthetic images, aiming to harness the strengths of each data source while mitigating their individual weaknesses.

On the issue of annotated data scarcity, self-supervised learning (SSL) has concurrently enjoyed significant advancements in recent years. The capability of unsupervised learning to generate high-quality features using pretext tasks now parallels, and in some cases surpasses, that of supervised learning. Even though SSL saves the annotation costs, the preparation of training data is still a vexing problem. Current research within SSL predominantly concentrates on the development of the pretext tasks, while the characteristics

of the data being utilized remain less explored. (Tian et al., 2023) uses text-conditional image generator for the creation of synthetic images, which are subsequently employed in the pre-training of an SSL model. This approach necessitates the use of image captions and a substantial dataset ( $\sim 20M$  images) to achieve performance parity with SSL models trained on real data. A training framework that uses synthetic images without any form of labels, prompts or huge amounts of training data, paired with real data has not been explored in the SSL setting before.

We ask the following question: Is it possible to improve SSL representations by combining both real and synthetic images using generative models in a fully self-supervised way? This paper answers this question in the affirmative and provide DiffMix, that explores the potential of combining synthetic images, generated by generative models without any labelled data, with real-world images for SSL training. We illustrate DiffMix in Figure 1. This approach aims to leverage the advantages of both data types: the controlled diversity of synthetic images and the authenticity of real-world data. We find that models pre-trained exclusively on synthetic images underperform compared to those pre-trained with real images across most scenarios. Interestingly, the combined pre-training approach using both real and synthetic images of DiffMix markedly boosts the performance of the same model, indicating superior learned representations. Additionally, DiffMix can work with virtually any model architecture with little modification, indicating that mixed pre-training strategy might be superior to conventional SSL pre-training methods.

We applied the mixing technique of DiffMix to various established SSL methods, including SimCLR(Chen et al., 2020), DINO (Caron et al., 2021), and BarlowTwins (Zbontar et al., 2021), and observed notable improvements in their performance. We complement the results with attributes of the generated synthetic images that we find are pivotal in how effectively the models learn and adapt to new datasets, particularly in aspects of robustness and adaptability. Contrary to the common belief that SSL performs better with high-quality real images, our research shows that lower quality synthetic images may contribute to stronger representations. Interestingly, we also discovered that image augmentations, typically beneficial for SSL, become somewhat unnecessary and even redundant in a mixed real and synthetic image setting. Through an analysis of various synthetic image qualities and their effects on the mixing process, we showcase new insights into optimizing SSL pre-training strategies. Our key contributions are:

- We introduce DiffMix, a new SSL pre-training framework, which facilitates the learning of cross real-synthetic image representations without any labels.
- The representations learned through DiffMix are found to be more adaptable than representations learned

from real images towards distribution shifts and various domain transfer tasks. We report up to 4.56% improvement on ImageNet-1K using SimCLR.

- We discover that lower-quality synthetic data leads to better mixing and superior performance. When trained without augmentation, DiffMix even surpasses SimCLR trained with heavy augmentation, suggesting synthetic data may replace augmentations in SSL.

## 2. Related Work

**Self-supervised Learning.** While SSL techniques exist in different forms, one of the most successful self-supervised learning paradigms is joint-embedding SSL (Misra & Maaten, 2020; He et al., 2020; Ye et al., 2019; Oord et al., 2018; Chen et al., 2020; Zbontar et al., 2021). The main focus of joint-embedding SSL is instance-based discriminative learning (Dosovitskiy et al., 2014; Assran et al., 2023), where each image is considered to be its own class, and a model is trained by discriminating different views of the same image generated using data augmentation (He et al., 2020; Chen et al., 2020; Zbontar et al., 2021; Caron et al., 2021). One such example is SimCLR (Chen et al., 2020), which uses an InfoNCE-based formulation (Oord et al., 2018) to bring in the representation of different views of the same image closer (‘positive pairs’), and repel representations of views from different images (‘negative pairs’) apart. In most cases, joint-embedding SSL methods work in a Siamese setting(Chen & He, 2021) where two branches have identical architectures and share weights. However, networks under such the Siamese setting are vulnerable to collapsing to trivial representations. BarlowTwins (Zbontar et al., 2021) brings covariance regularization to the contrastive setting as a to enforce a non-collapsing solution. More recently, works such as DINO (Caron et al., 2021) have shown alternative ways to prevent collapse using architectural strategies inspired by knowledge distillation (Hinton et al., 2015). In this work, we provide an improved pre-training mechanism for representation learning in such joint-embedding SSL techniques.

**Learning using Synthetic Data.** Recent advancements in machine learning have increasingly leveraged synthetic data across a variety of domains (Silver et al., 2017; Mimura et al., 2018; Meng et al., 2022; Dan et al., 2019). This type of data is particularly crucial for tasks that demand extensive labeled datasets, such as human pose estimation (Ma et al., 2022; Guo et al., 2022), semantic segmentation (Chen et al., 2018; Rewatbowornwong et al., 2021), and optical flow estimation (whan Kim et al., 2022; Sun et al., 2021). In the task of image classification, several studies have demonstrated the effectiveness of synthetic data. (He et al., 2022b) illustrates its application in data-scarce settings and transfer learning; (Wang et al., 2023) explores its role in enhancing adversarial

training; (Bansal & Grover, 2023; Sariyildiz et al., 2022) evaluates model robustness against natural distribution shifts using synthetic data; and (Azizi et al., 2023) discusses augmentation of images through fine-tuned text-to-image diffusion models. It is important to note that all of these studies focus on supervised learning. Our work, however, is distinct in its concentration on SSL and additionally investigates both robustness and transfer learning. The study most closely aligned with our research is that of (Tian et al., 2023), which utilizes text-to-image diffusion models for generating images, often producing multiple images from a single caption. In contrast, our approach employs image-to-image diffusion models and is designed to generate only one image for each source image. This method reduces the reliance on labeled data for image generation and the cost of image generation.

**Generative Models.** The landscape of synthetic image generation has seen a significant evolution, with Generative Adversarial Networks (GANs) such as BigGAN (Brock et al., 2018) initially setting a high standard. These models have been pivotal in pushing the boundaries of image realism and quality. Recently, diffusion models have emerged as a promising alternative, demonstrating impressive results in both conditional (Dhariwal & Nichol, 2021; Saharia et al., 2021) and unconditional (Ho et al., 2021) synthetic image generation. Text-to-image diffusion models like DALL-E (Ramesh et al., 2021) and Imagen (Saharia et al., 2022) are notable examples, showcasing the ability to create detailed and contextually accurate images from textual descriptions. Our research takes a unique turn by focusing on the image-to-image diffusion model, specifically a fine-tuned version of Stable Diffusion (Rombach et al., 2021). This model distinguishes itself by utilizing CLIP (Radford et al., 2021) image embeddings instead of text embeddings.

### 3. Method

In this work, we primarily focus on Self-Supervised Learning (SSL) techniques, particularly those that consolidate representations from different perspectives or augmentations of the same instance (Alexey et al., 2016; Wu et al., 2018; He et al., 2020; Chen et al., 2020). The main idea behind this technique is, through iterative processes, these representations gradually become less sensitive to the transformations generating these varied views. Consequently, this leads to the learning of image representations that are notably effective for vision tasks such as classification (He et al., 2020; Chen et al., 2020; Zbontar et al., 2021). In this section, we introduce our framework, DiffMix, which uniquely employs both real and synthetically generated data through stable diffusion, and see how it can be incorporated in some of the existing SSL frameworks.

#### 3.1. Description of DiffMix

Consider  $x_1$  and  $x'_1$ , two augmented patches from an image, randomly selected from a dataset. These augmentations can include a variety of changes, such as altering spatial positions within an image, adding varying noise and applying random color adjustments, etc. Existing instance-based discriminative SSL methods primarily rely on real images (He et al., 2020; Chen et al., 2020; Zbontar et al., 2021; Caron et al., 2021). In these methods, the representation derived from the first augmentation,  $x_1$ , of a real image is anticipated to closely align with the representation of the second augmentation,  $x'_1$ , of the same image as shown in Figure 1. Our DiffMix framework modifies this approach by incorporating synthetically generated images alongside real ones. The primary objective of DiffMix is to synchronize the representations of real and synthetic images, thus enhancing existing SSL methodologies such as SimCLR, DINO, and BarlowTwins.

The synthetic images employed by DiffMix have a unique characteristic that they share a variation of the same semantic component or object with that of the real image. To achieve this, we employ Image Variation Diffuser<sup>1</sup>, a variant of Stable Diffusion (Rombach et al., 2021) tailored to generate diverse images while preserving semantic categories or in simple terms, the image class. In the Stable Diffusion-based generative model, represented as  $g_{SD}^k(\cdot)$ , where  $k$  indicates the guidance scale influencing the generative features from the input image, an input  $x_i \sim D$  yields a synthetic counterpart  $\tilde{x}_i$ , such that  $\tilde{x}_i = g_{SD}^k(x_i)$ . The innovative aspect of DiffMix lies in substituting a portion of the augmentation process, i.e, the second branch of augmentation  $x'_i$  within the SSL framework with these synthetic images  $\tilde{x}_i$ , to learn cross real-synthetic image representations as shown in Figure 1.

#### 3.2. Mixing in joint-embedding SSL

**SimCLR + DiffMix:** In SimCLR’s contrastive learning framework (Chen et al., 2020), ‘positive’ and ‘negative’ pairs of images are identified, with the goal of either converging or diverging their representations. In SimCLR, two augmented views are generated for each image in a mini-batch, resulting in  $2N$  images for a mini-batch size of  $N$ . Each view is paired with its corresponding alternate view as a ‘positive’ pair, while the remaining  $2(N-1)$  images are treated as ‘negative’ pairs. We now propose to incorporate *mixing* into SimCLR. We first define a new set  $\{x_k, \tilde{x}_k\}$  for  $k \in [1, 2, \dots, N]$ , where  $\tilde{x}_k$  denotes the synthetically generated counterpart of  $x_k$ , thus establishing pairs like  $x_1$  and  $\tilde{x}_1$  as positive examples. The contrastive prediction task of the modified, which we term as SimCLR+DiffMix now involves identifying  $x_1$  and  $\tilde{x}_1$  in  $\{x_k, \tilde{x}_k\} \forall k \in [1, N]$ . The modified loss function for the mixed version of SimCLR, denoted as  $\mathcal{L}_{MixSR}$ , for a

<sup>1</sup><https://huggingface.co/lambdalabs/sd-image-variations-diffusers>

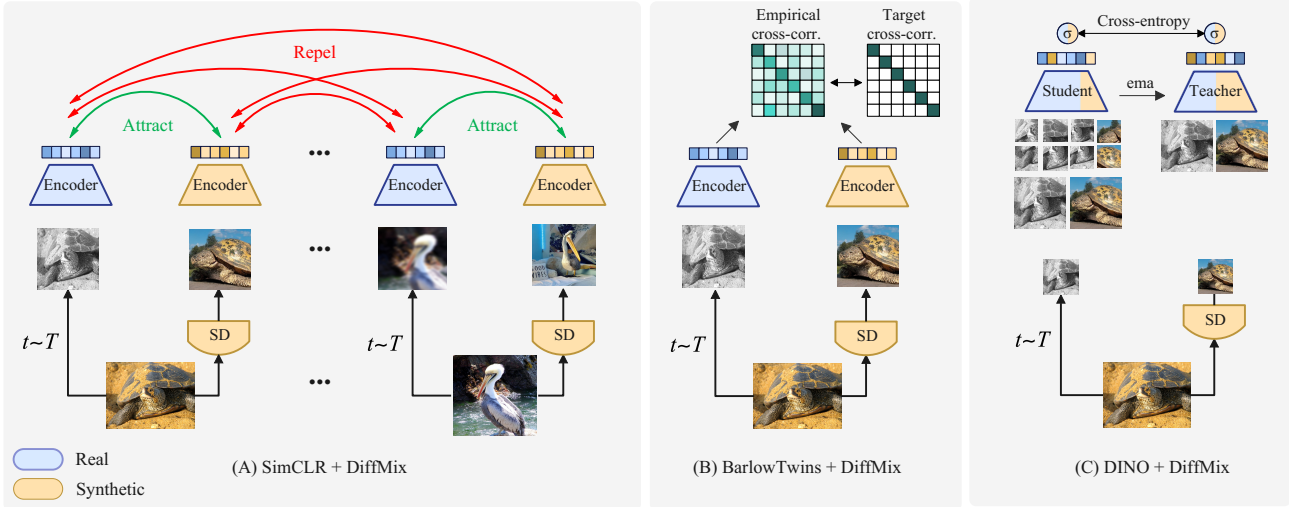


Figure 2. Existing SSL methods, including (A) SimCLR, (B) Barlow Twins, and (C) DINO, have been enhanced with our novel DiffMix approach. In both (A) SimCLR and (B) Barlow Twins, we replace a branch representing the positive pair with a synthetic image generated without the label using Stable Diffusion. This modification enables the learning of real-synthetic view prediction. (C) DINO utilizes a distillation framework with two global views for the teacher and a mix of two global and eight local views for the student. Our adaptation integrates an equal blend of global and local synthetic and real images facilitating learning correspondences between global-to-local on top of real-to-synthetic image views.

positive pair of examples  $(x_i, \tilde{x}_i)$ , is defined as:

$$\mathcal{L}_{MixSR}^i \triangleq -\log \frac{\exp(\text{sim}(z_i, \tilde{z}_i)) / \tau}{\sum_{z \in \{z_j, \tilde{z}_j, \forall j \in [1, N]\}} \mathbb{1}_{z \neq z_i, \tilde{z}_i} \exp(\text{sim}(z_i, z))}$$

where for a given two feature vectors,  $u$  and  $v$ , their ‘sim’ refers to the cosine similarity and is calculated as  $\text{sim}(u, v) = \frac{u^T v}{\|u\| \|v\|}$ , representing the dot product of the  $l_2$  normalized vectors  $u$  and  $v$ . And  $z_i$  and  $\tilde{z}_i$  are the outputs of the network  $f(\cdot)$  we are developing, expressed as:

$$z_i = f(x_i) \text{ and } \tilde{z}_i = f(\tilde{x}_i) = f(g_{SD}^k(x_i))$$

While the original SimCLR focuses on aligning representations of variously distorted versions of the same real image, our modified approach aims to align representations of a real image with its synthetic counterpart generated by Stable Diffusion as shown in Figure 2 (A). Concurrently, we strive to differentiate these pairs from other real and synthetic image pairs.

**Barlow Twins + DiffMix:** The Barlow Twins framework (Zbontar et al., 2021), while maintaining a Siamese network structure similar to SimCLR (Chen et al., 2020), adopts a distinct approach to representation alignment. The difference lies in the Barlow Twins’ objective function, which assesses the cross-correlation matrix between the embeddings from two identical networks. These networks process distorted versions of a batch of samples, with the aim of aligning this matrix closely with the identity matrix. This

alignment ensures that the embeddings of distorted versions of a sample are similar, while simultaneously reducing redundancy among the components of these embeddings.

In our modified approach, as we show in Figure 2 (B), we innovate by introducing a synthetic element into this framework. Instead of solely using distorted versions of the same real image, we integrate a distorted version of a synthetic image. Following the notation from the previous section, let  $z_i$  represent the distorted version of a real image and  $\tilde{z}_j$  that of a synthetic image. The objective function for this adapted version of Barlow Twins, denoted as  $\mathcal{L}_{BT}$ , is formulated as:

$$\mathcal{L}_{BT} \triangleq \sum_i (1 - C_{ii})^2 + \lambda \sum_i \sum_{j \neq i} C_{ij}^2$$

Here,  $\lambda$  is a positive constant that balances the first and second terms in the loss function. The cross-correlation matrix,  $\mathcal{C}$ , is computed between the outputs of the two identical networks, one fed with real images and the other with synthetic images, as follows:

$$C_{ij} \triangleq \frac{\sum_b z_{b,i} \tilde{z}_{b,j}}{\sqrt{\sum_b (z_{b,i})^2} \sqrt{\sum_b (\tilde{z}_{b,j})^2}}$$

where  $b$  indexes the batch samples, while  $i$  and  $j$  index the vector dimensions of the networks’ outputs. This updated approach, which integrates synthetic images into the Barlow Twins framework, focuses on aligning the representations of real ( $z_i$ ) and synthetic images ( $\tilde{z}_j$ ) via the cross-correlation matrix. We give more details regarding mixing in joint-embedding SSL in the Appendix B.

### 3.3. Mixing in Distillation SSL

**DINO + DiffMix:** The DINO model processes images using a multi-crop strategy to create multiple views at different scales, including two high-resolution global views ( $x_1^g, x_2^g$ ) and multiple lower-resolution local views ( $x_k^l, k=1$  to 8). It employs a knowledge distillation (KD) framework where a student network  $g_{\theta_s}$  learns to match the output of a teacher network  $g_{\theta_t}$ , with the student processing both local and global views, while the teacher focuses on global views to enhance 'local-to-global' learning. Building on this foundation, we introduce image mixing in DINO, termed DINO + DiffMix, the model is adapted to integrate both real and synthetic images. This is accomplished by adjusting the view composition to include one global and six local views from a real image, plus one global and two local views from a synthetic image. Consequently, our modified set includes a global view from a real image ( $x_1^g$ ), a global view from a synthetic image ( $\tilde{x}_2^g$ ), and four local views each from the real ( $x_r^l \forall r \in [1,6]$ ) and synthetic ( $\tilde{x}_q^l \forall q \in [1,2]$ ) images.

With a student network  $g(\theta_s)$  and a fixed teacher network  $g_{\theta_t}$  (updated via  $EMA^2$ ), the learning objective is to align these distributions. This is achieved by minimizing the cross-entropy loss with respect to the student network's parameters  $\theta_s$ , expressed as:  $\min_{\theta_s} H(P_t(X_t), P_s(X_s))$  where  $H(a,b) = -\log b$  denotes the cross-entropy function. Both the student and teacher networks generate probability distributions denoted as  $P_s$  and  $P_t$ , respectively, derived by normalizing the networks' outputs using a softmax function. This learning process involves passing all crops through the student network, while the teacher network processes only the global views. This design fosters 'local-to-global' as well as 'real-to-synthetic' learning correspondences. The loss objective becomes:

$$\min_{\theta_s} \sum_{X_t \in \{x_1^g, \tilde{x}_2^g\}} \sum_{X_s \in \tilde{V}, X_s \neq X_t} H(P_t(X_t), P_s(X_s))$$

We provide more details regarding mixing in distillation SSL such as DINO in Appendix C.1.

## 4. Experiments

In this section, we evaluate the representations obtained across different SSL techniques using DiffMix mentioned in Section 3 with configurations provided in Appendix D. We present experiments testing robustness to distribution shifts, domain transfer across datasets, and performance on low-quality images, assessing the learned representations.

**Training Datasets.** The substantial size of the ImageNet-1K (IN-1K) (Deng et al., 2009) dataset, which contains approximately 1.3 million images, presents challenges for extensive experimentation. Consequently, we primarily utilize

the more manageable ImageNet-100 (IN-100) dataset (Tian et al., 2019) for our studies, which include 100 classes and 1300 images per class. This dataset's smaller scale enables us to efficiently run multiple variations of each synthetic dataset and thoroughly evaluate the impact of various design choices. Nonetheless, we extend our experiments to IN-1K with SimCLR to validate our findings on a larger scale.

### 4.1. Robustness to distribution shifts

To evaluate performance under domain shifts, we selected a variety of datasets including ImageNet-A (IN-A) (Hendrycks et al., 2019), ImageNet-Sketch (IN-Sketch) (Wang et al., 2019), ObjectNet (Barbu et al., 2019), ImageNet-V2 (IN-V2) (Recht et al., 2019), and ImageNet-R (IN-R) (Hendrycks et al., 2020). We trained variants of DINO, SimCLR, and Barlow Twins models using real, synthetic, and a blend of both image types from the IN-100 dataset.

A key aspect of our methodology is the training of linear probes: they are consistently trained on real images from the same dataset as the model. For instance, models trained with synthetic IN-100 images use real IN-100 images for linear probe training. To train models on IN-100 we used subsets of the datasets with common categories with IN-100 (ObjectNet was excluded due to lack of common labels with IN-100).

Models leveraging DiffMix exhibit higher accuracy on the IN-100 and other datasets, compared to models trained solely on real or synthetic images (Table 1). This indicates that DiffMix enhances robustness to natural distribution shifts.

In Table 3, we drill down on the SimCLR variants on the IN-1K dataset, and these findings align with our previous observations from the IN-100 dataset. While DINO outperforms on IN-100, we chose SimCLR for this experiment owing to its markedly quicker training time, attributed to its use of fewer crops and simpler data augmentations.

Notably, the model trained with DiffMix exhibits superior performance compared to those trained solely on either type. This advantage is consistent across various natural distribution datasets. However, it is crucial to highlight that accuracy on more challenging datasets like ImageNet-A is still low (Tomasev et al., 2022; Djolonga et al., 2020). This may be attributed to the backbone of the SimCLR model being ResNet-50, while ImageNet-A was curated specifically as images that fool the ResNet-50 model (Hendrycks et al., 2019).

### 4.2. Domain transfer on different datasets

Our models' feature generality was assessed by testing their performance across different image domains, using a wide range of datasets to evaluate DiffMix's effectiveness. The datasets include: Aircraft (Maji et al., 2013), DTD (Describable Textures Dataset) (Cimpoi et al., 2013), Flowers102 (Nilsback & Zisserman, 2008), Food101

<sup>2</sup>EMA: Exponential Moving Average

Table 1. Top-1 classification accuracies (%) for various models on ImageNet-100 domain shift datasets. This table compares the performance of models trained on real, synthetic (Syn), and an equal combination of real and synthetic (DiffMix) images.

MODEL	IN-100	IN-V2	IN-SKETCH	IN-A	IN-R	MEAN
SIMCLR	66.56	59.80	15.12	9.00	31.52	36.40
SIMCLR+SYN	61.00 (-5.56)	52.50 (-7.30)	14.55 (-0.57)	8.43 (-0.41)	29.77 (-1.75)	33.25 (-3.15)
SIMCLR+DIFFMIX	73.30 (+6.74)	66.30 (+6.50)	<b>21.27 (+6.15)</b>	11.13 (+2.13)	<b>44.02 (+12.50)</b>	43.20 (+6.08)
DINO	66.76	57.90	10.13	8.52	27.46	34.15
DINO+SYN	61.38 (-5.38)	54.30 (-3.6)	8.68 (-1.45)	7.49 (-1.03)	27.97 (+0.51)	31.96 (-2.19)
DINO+DIFFMIX	<b>77.96 (+11.20)</b>	<b>70.20 (+12.30)</b>	18.89 (+8.76)	<b>12.85 (+4.33)</b>	37.50 (+10.04)	<b>43.48 (+9.33)</b>
BARLOW	68.10	62.90	12.25	8.12	31.14	36.50
BARLOW+SYN	58.62 (-9.48)	53.30 (-9.60)	9.49 (-2.76)	7.02 (-1.10)	26.30 (-4.84)	30.95 (-5.56)
BARLOW+DIFFMIX	72.02 (+3.92)	64.40 (+1.50)	16.38 (+4.13)	9.42 (+1.30)	38.71 (+7.57)	40.19 (+3.68)

Table 2. Comparison of different configurations of the DINO model and their top-1 accuracy on the IN-100 validation dataset. The first row presents the original settings. Columns represent the number of local (#L) and global (#G) views.

DIFFMIX	REAL		SYN		ACC.
	#L	#G	#L	#G	
×	8	2	-	-	66.75
×	-	-	8	2	61.38
✓	2	1	6	1	77.43
✓	4	1	4	1	77.52
✓	6	1	2	1	<b>77.96</b>

(Bossard et al., 2014), CIFAR-10 (Krizhevsky, 2009), and CIFAR-100 (Krizhevsky, 2009).

We leveraged the SimCLR model, training it on a mix of real, synthetic, and DiffMix data within the IN-1K dataset. For each variant, we first pre-trained SimCLR’s backbone, subsequently freezing these pre-trained layers to focus on training linear probes. The top-1 accuracy results for each dataset variation are presented in Table 4. These findings demonstrate our approach’s superiority in achieving higher top-1 accuracy across all datasets, surpassing models trained solely on real or synthetic images. For a fair comparison, we standardized the evaluation by using the same SimCLR hyperparameters for all variations. Although our training iterations are lower (100 epochs) as compared to the original SimCLR (1000 epochs), resulting in slightly lower numbers, our method still consistently outperforms the original SimCLR model in relative terms.

### 4.3. Performance on low-quality images

In this section, we assess the performance of our pre-trained models on the IN-1K dataset, using the VizWiz-Classification (VW-C) dataset (Bafghi & Gurari, 2023). This dataset is notable for containing images taken by people who are blind with various quality issues, such as blur, underexposure, overexposure, poor framing, obscured, and rotated views. We

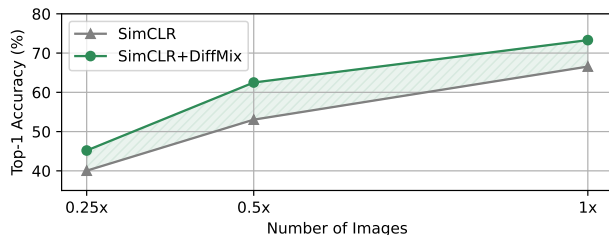


Figure 3. Comparison of top-1 accuracy on IN-100 for SimCLR models trained with and without DiffMix across varying scales of training images. The green shaded area indicates the performance gap between the two models.

evaluate model performance on corrupted (the mean accuracy of six quality issues), clean, and all images of the dataset.

Table 5 outlines our results. Interestingly, the model trained only on synthetic data, which typically have lower quality, exhibits a smaller drop in accuracy on corrupted images (0.08%) than seen with the clean images of VW-C (2.05%) and the ImageNet validation dataset (6.06%). Finally, our framework can enhance SimCLR models’ ability to manage images with quality issues, highlighting its practical value in real-world scenarios where image quality can vary.

### 4.4. Training with limited data

We explored the impact of limited data on SSL, assessing DiffMix’s effectiveness. Using 25%, 50%, and 100% of the IN-100 dataset and synthetic images generated with a guidance scale of 8, we trained SimCLR models on both original and DiffMix-augmented images. Linear probes were trained on the real images of each subset. Results show that performance gains persist, with a 5.14% increase even when training on only 25% of the images.

## 5. Ablation study of DiffMix

In this section, we empirically study DiffMix applied to SimCLR and DINO, focusing on finding the optimal

Table 3. Top-1 classification accuracies (%) of various models trained on ImageNet-1K, evaluated on domain shift datasets.

MODEL	IN-1K	IN-V2	IN-SKETCH	IN-A	IN-R	OBJECTNET	MEAN
SIMCLR	63.34	50.10	14.08	1.64	23.71	14.64	27.92
SIMCLR+SYN	57.58	44.70	16.19	1.72	26.12	11.35	26.28
SIMCLR+DIFFMIX	<b>67.90</b>	<b>54.53</b>	<b>22.57</b>	<b>2.22</b>	<b>34.97</b>	<b>19.65</b>	<b>33.64</b>

Table 4. Comparison of transfer learning performance on six diverse datasets for models trained on ImageNet-1K.

MODEL	CIFAR-10	CIFAR-100	AIRCRAFT	DTD	FLOWERS102	FOOD101	MEAN
SIMCLR	72.80	47.11	18.99	57.28	73.13	64.05	55.56
SIMCLR+SYN	71.04	44.36	17.94	51.80	69.02	58.06	52.04
SIMCLR+DIFFMIX	<b>77.90</b>	<b>53.02</b>	<b>24.36</b>	<b>58.59</b>	<b>82.94</b>	<b>66.40</b>	<b>60.53</b>

Table 5. Accuracies of models trained on ImageNet-1K, evaluated on corrupted, clean, and all images of VW-C.

MODEL	CORRUPTED	CLEAN	MEAN
SIMCLR	18.87	30.16	24.96
SIMCLR+SYN	18.79	28.11	23.25
SIMCLR+DIFFMIX	<b>23.94</b>	<b>35.02</b>	<b>29.93</b>

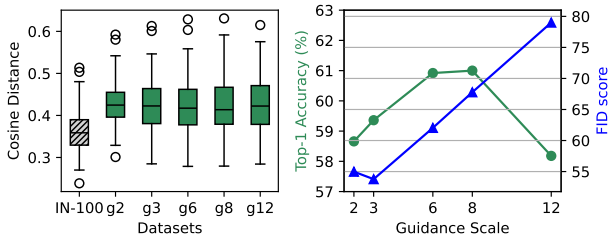


Figure 4. **Left:** Distribution of mean cosine distance between feature vectors of images of all categories of IN-100 and generated images with different guidance scales. **Right:** The relationship between guidance scales used in image generation and the corresponding FID scores of the generated images (Blue line). Additionally, it shows the top-1 accuracy of SimCLR models when trained only on synthetic images, evaluated on the ImageNet-100 dataset (Green line).

guidance scale, understanding the effect of mixing levels on accuracy and self-attention mask, and evaluating the impact of data augmentation on model performance.

### 5.1. Existence of optimal guidance scale

In our study, we aimed to identify the optimal guidance scale for generating images on IN-100, which could then be applied to larger-scale image generation for IN-1K. This follows the methodology outlined in (Tian et al., 2023). As demonstrated in Figure 4, we found that using a guidance scale of 8 yields the highest top-1 accuracy on the IN-100 validation dataset. This finding is consistent with the results from (Tian et al., 2023), despite our use of different

generative models and image generation approaches. We plot the Frechet Inception Distance (FID) scores (Heusel et al., 2017) to assess the similarity between generated images and IN-100 source images across guidance scales. Interestingly, in general, we observe an inverse relationship between accuracy and image quality. Additionally, in the Left Figure 4, following (Bafghi & Gurari, 2023), we calculate the mean cosine distances between all feature vector pairs per category using CLIP (Radford et al., 2021) for feature extraction, demonstrating that generated images offer more diversity than real images. This diversity may be attributed to the randomness introduced by our generative model.

### 5.2. DINO: Impact of mixing in self-attention

In our analysis of DINO (Caron et al., 2021) models trained on IN-100, we interpret masks derived from self-attention maps by applying thresholds for enhanced visualization. These maps, sourced from the top-performing head of each ViT-S/16 (Dosovitskiy et al., 2020) DINO model trained on both real and synthetic ImageNet datasets using our DiffMix approach, are not designed for mask creation but rather to highlight the model’s focus areas during image processing. Our findings, illustrated in Figure 5, show that models trained on real images effectively segment objects with some background attention. In contrast, the model trained on synthetic images shows a tendency to focus less on the background, but the overall object segmentation appears somewhat less defined. The DiffMix-trained model strikes a balance, demonstrating clearer object focus with minimal background distraction, indicating improved object segmentation. This improvement is clearly visible in the last row of Figure 5. This suggests that integrating synthetic data with the DiffMix method may enhance scene understanding and image segmentation capabilities.

### 5.3. Performance trend with varying mixing levels

We explore various configurations of image splitting between real and synthetic images for the DINO model. DINO utilizes

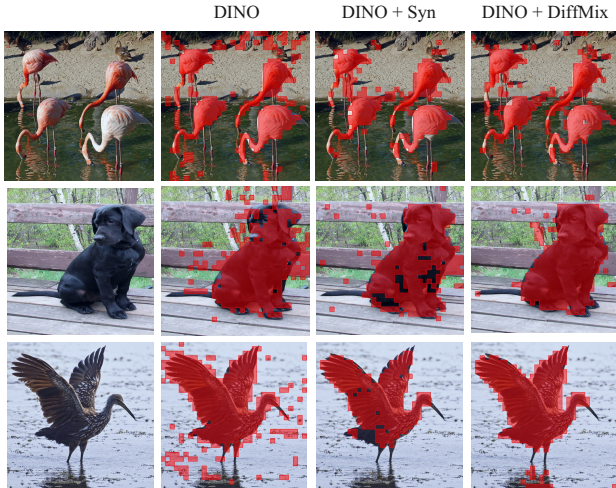


Figure 5. We present the masks generated by applying a 65% threshold to the self-attention maps. The above maps were obtained using the best head from each ViT-S/16 DINO model that has been trained on ImageNet-100 using real and synthetically generated ImageNet versus DiffMix.

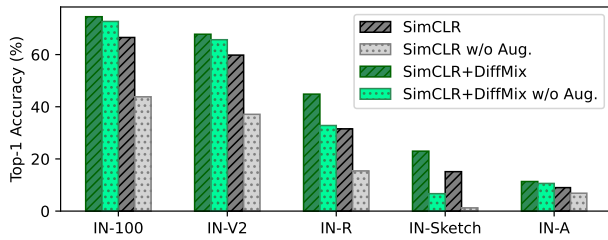


Figure 6. Top-1 accuracy comparison of SimCLR models trained with and without DiffMix, and the impact of including versus omitting SSL data augmentations.

a total of 10 crops: the teacher model processes two global crops, while the student model analyzes eight local views in addition to the global views. Figure 2 presents a comparison of different configurations and their corresponding top-1 accuracy on the IN-100 validation dataset. All synthetic images are generated with a guidance scale of 8.

The findings demonstrate that dividing the training dataset into a mix of real and synthetic images can enhance accuracy, and our framework shows robustness to varying proportions of these images. The most effective configuration identified involves using 2 local views and 1 global view from synthetic images, along with 6 local views and 1 global view from real images. This specific arrangement yielded the highest top-1 accuracy, reaching 78.24%.

#### 5.4. Impact of Data Augmentation

Our study investigates the effect of data augmentation on the SimCLR model, comparing its performance when trained

with DiffMix versus solely real images of IN-100. Specifically, for models trained without augmentation, we retain only the random flip and eliminate all other augmentations.

As depicted in Figure 6, an interesting finding is that omitting data augmentations—a key component in self-supervised learning models—does not significantly affect the performance of models trained with both real and synthetic images. The DiffMix model without augmentation generally surpasses the original SimCLR, except for the ImageNet-Sketch dataset. Conversely, in stark contrast, SimCLR models trained exclusively on real images experience a pronounced accuracy decrease in the absence of data augmentations. Specifically, the average accuracy drop across five validation datasets is 15.52% for SimCLR without augmentation, compared to a lesser accuracy drop of 6.60% for SimCLR+DiffMix. Notably, removing these augmentations can lead to faster training times, which is significant considering that data augmentations are often a major bottleneck in the training process, as highlighted in (Bordes et al., 2023).

## 6. Conclusion

This work demonstrates the potential of mixing synthetic images generated without any labels, with real images in self-supervised pretraining. When used across existing SSL techniques, DiffMix consistently improves the methods across various benchmarks, without any extra data. We identify several properties that could be exploited in future works leveraging synthetic images in SSL. Lower-quality synthetic images from Stable Diffusion can lead to better representations when compared with higher-quality images of the same resolution. Mixing synthetic data with real images can serve as an alternative to augmentations in current SSL methods, proving especially beneficial in domains where applying augmentations is challenging. We further discover that mixing of synthetic data in models like DINO could result in less emphasis on the background, hinting at an enhanced understanding of scene layout within the features that can be leveraged for image segmentation.

Our research reveals a noticeable performance gap between models trained solely on synthetic images and those trained on actual images. This indicates a significant unexplored potential in the development of generative models to improve efficiency and produce images that more closely mimic the distribution of real images. In future work we aim to investigate advanced generative diffusion models that could facilitate better mixing and enhance the robustness of visual features.

## References

Alexey, D., Fischer, P., Tobias, J., Springenberg, M. R., and Brox, T. Discriminative unsupervised feature learning with exemplar convolutional neural networks. *IEEE*



- TPAMI*, 38(9):1734–1747, 2016.
- Assran, M., Duval, Q., Misra, I., Bojanowski, P., Vincent, P., Rabbat, M., LeCun, Y., and Ballas, N. Self-supervised learning from images with a joint-embedding predictive architecture. In *Proceedings of the IEEE/CVF Conference on Computer Vision and Pattern Recognition*, pp. 15619–15629, 2023.
- Azizi, S., Kornblith, S., Saharia, C., Norouzi, M., and Fleet, D. J. Synthetic data from diffusion models improves imagenet classification. *ArXiv*, abs/2304.08466, 2023. URL <https://api.semanticscholar.org/CorpusID:258179174>.
- Bafghi, R. A. and Gurari, D. A new dataset based on images taken by blind people for testing the robustness of image classification models trained for imagenet categories. *2023 IEEE/CVF Conference on Computer Vision and Pattern Recognition (CVPR)*, pp. 16261–16270, 2023. URL <https://api.semanticscholar.org/CorpusID:260813958>.
- Bansal, H. and Grover, A. Leaving reality to imagination: Robust classification via generated datasets. *ArXiv*, abs/2302.02503, 2023. URL <https://api.semanticscholar.org/CorpusID:256616163>.
- Barbu, A., Mayo, D., Alverio, J., Luo, W., Wang, C., Gutfreund, D., Tenenbaum, J. B., and Katz, B. Objectnet: A large-scale bias-controlled dataset for pushing the limits of object recognition models. In *Neural Information Processing Systems*, 2019. URL <https://api.semanticscholar.org/CorpusID:202777185>.
- Bordes, F., Balestrieri, R., and Vincent, P. Towards democratizing joint-embedding self-supervised learning. *ArXiv*, abs/2303.01986, 2023. URL <https://api.semanticscholar.org/CorpusID:257353289>.
- Bossard, L., Guillaumin, M., and Gool, L. V. Food-101 - mining discriminative components with random forests. In *European Conference on Computer Vision*, 2014. URL <https://api.semanticscholar.org/CorpusID:12726540>.
- Brock, A., Donahue, J., and Simonyan, K. Large scale gan training for high fidelity natural image synthesis. *ArXiv*, abs/1809.11096, 2018. URL <https://api.semanticscholar.org/CorpusID:52889459>.
- Caron, M., Touvron, H., Misra, I., Jégou, H., Mairal, J., Bojanowski, P., and Joulin, A. Emerging properties in self-supervised vision transformers. In *Proceedings of the IEEE/CVF international conference on computer vision*, pp. 9650–9660, 2021.
- Chen, T., Kornblith, S., Norouzi, M., and Hinton, G. A simple framework for contrastive learning of visual representations. In *International conference on machine learning*, pp. 1597–1607. PMLR, 2020.
- Chen, X. and He, K. Exploring simple siamese representation learning. In *Proceedings of the IEEE/CVF conference on computer vision and pattern recognition*, pp. 15750–15758, 2021.
- Chen, Y., Li, W., Chen, X., and Gool, L. V. Learning semantic segmentation from synthetic data: A geometrically guided input-output adaptation approach. *2019 IEEE/CVF Conference on Computer Vision and Pattern Recognition (CVPR)*, pp. 1841–1850, 2018. URL <https://api.semanticscholar.org/CorpusID:54474202>.
- Cimpoi, M., Maji, S., Kokkinos, I., Mohamed, S., and Vedaldi, A. Describing textures in the wild. *2014 IEEE Conference on Computer Vision and Pattern Recognition*, pp. 3606–3613, 2013. URL <https://api.semanticscholar.org/CorpusID:4309276>.
- Dan, Y., Zhao, Y., Li, X., Li, S., Hu, M., and Hu, J. Generative adversarial networks (gan) based efficient sampling of chemical composition space for inverse design of inorganic materials. *npj Computational Materials*, 6:1–7, 2019. URL <https://api.semanticscholar.org/CorpusID:220065333>.
- Deng, J., Dong, W., Socher, R., Li, L.-J., Li, K., and Fei-Fei, L. Imagenet: A large-scale hierarchical image database. *2009 IEEE Conference on Computer Vision and Pattern Recognition*, pp. 248–255, 2009. URL <https://api.semanticscholar.org/CorpusID:57246310>.
- Dhariwal, P. and Nichol, A. Diffusion models beat gans on image synthesis. *ArXiv*, abs/2105.05233, 2021. URL <https://api.semanticscholar.org/CorpusID:234357997>.
- Djulonga, J., Yung, J., Tschannen, M., Romijnders, R., Beyer, L., Kolesnikov, A., Puigcerver, J., Minderer, M., D’Amour, A., Moldovan, D. I., Gelly, S., Houlsby, N., Zhai, X., and Lucic, M. On robustness and transferability of convolutional neural networks. *2021 IEEE/CVF Conference on Computer Vision and Pattern Recognition (CVPR)*, pp. 16453–16463, 2020. URL <https://api.semanticscholar.org/CorpusID:220633571>.
- Dosovitskiy, A., Springenberg, J. T., Riedmiller, M., and Brox, T. Discriminative unsupervised feature learning with convolutional neural networks. *Advances in neural information processing systems*, 27, 2014.

- Dosovitskiy, A., Beyer, L., Kolesnikov, A., Weissenborn, D., Zhai, X., Unterthiner, T., Dehghani, M., Minderer, M., Heigold, G., Gelly, S., Uszkoreit, J., and Houlsby, N. An image is worth 16x16 words: Transformers for image recognition at scale. *ArXiv*, abs/2010.11929, 2020. URL <https://api.semanticscholar.org/CorpusID:225039882>.
- Goodfellow, I., Pouget-Abadie, J., Mirza, M., Xu, B., Warde-Farley, D., Ozair, S., Courville, A., and Bengio, Y. Generative adversarial nets. *Advances in neural information processing systems*, 27, 2014.
- Grill, J.-B., Strub, F., Althé, F., Tallec, C., Richemond, P., Buchatskaya, E., Doersch, C., Avila Pires, B., Guo, Z., Gheshlaghi Azar, M., et al. Bootstrap your own latent—a new approach to self-supervised learning. *Advances in neural information processing systems*, 33:21271–21284, 2020.
- Guo, X., Wu, W., Wang, D., Su, J., Su, H., Gan, W., Huang, J., and Yang, Q. Learning video representations of human motion from synthetic data. *2022 IEEE/CVF Conference on Computer Vision and Pattern Recognition (CVPR)*, pp. 20165–20175, 2022. URL <https://api.semanticscholar.org/CorpusID:252576035>.
- He, K., Fan, H., Wu, Y., Xie, S., and Girshick, R. Momentum contrast for unsupervised visual representation learning. In *Proceedings of the IEEE/CVF conference on computer vision and pattern recognition*, pp. 9729–9738, 2020.
- He, R., Sun, S., Yu, X., Xue, C., Zhang, W., Torr, P., Bai, S., and Qi, X. Is synthetic data from generative models ready for image recognition? *arXiv preprint arXiv:2210.07574*, 2022a.
- He, R., Sun, S., Yu, X., Xue, C., Zhang, W., Torr, P. H. S., Bai, S., and Qi, X. Is synthetic data from generative models ready for image recognition? *ArXiv*, abs/2210.07574, 2022b. URL <https://api.semanticscholar.org/CorpusID:252907242>.
- Hendrycks, D., Zhao, K., Basart, S., Steinhardt, J., and Song, D. X. Natural adversarial examples. *2021 IEEE/CVF Conference on Computer Vision and Pattern Recognition (CVPR)*, pp. 15257–15266, 2019. URL <https://api.semanticscholar.org/CorpusID:196831327>.
- Hendrycks, D., Basart, S., Mu, N., Kadavath, S., Wang, F., Dorundo, E., Desai, R., Zhu, T. L., Parajuli, S., Guo, M., Song, D. X., Steinhardt, J., and Gilmer, J. The many faces of robustness: A critical analysis of out-of-distribution generalization. *2021 IEEE/CVF International Conference on Computer Vision (ICCV)*, pp. 8320–8329, 2020. URL <https://api.semanticscholar.org/CorpusID:220250257>.
- Heusel, M., Ramsauer, H., Unterthiner, T., Nessler, B., and Hochreiter, S. Gans trained by a two time-scale update rule converge to a local nash equilibrium. In *Neural Information Processing Systems*, 2017. URL <https://api.semanticscholar.org/CorpusID:326772>.
- Hinton, G., Vinyals, O., and Dean, J. Distilling the knowledge in a neural network. *arXiv preprint arXiv:1503.02531*, 2015.
- Ho, J., Jain, A., and Abbeel, P. Denoising diffusion probabilistic models. *Advances in neural information processing systems*, 33:6840–6851, 2020.
- Ho, J., Saharia, C., Chan, W., Fleet, D. J., Norouzi, M., and Salimans, T. Cascaded diffusion models for high fidelity image generation. *J. Mach. Learn. Res.*, 23:47:1–47:33, 2021. URL <https://api.semanticscholar.org/CorpusID:235619773>.
- Jeelani, M., Cheema, N., Illgner-Fehns, K., Slusallek, P., Jaiswal, S., et al. Expanding synthetic real-world degradations for blind video super resolution. In *Proceedings of the IEEE/CVF Conference on Computer Vision and Pattern Recognition*, pp. 1199–1208, 2023.
- Krizhevsky, A. Learning multiple layers of features from tiny images. 2009. URL <https://api.semanticscholar.org/CorpusID:18268744>.
- Langley, P. Crafting papers on machine learning. In Langley, P. (ed.), *Proceedings of the 17th International Conference on Machine Learning (ICML 2000)*, pp. 1207–1216, Stanford, CA, 2000. Morgan Kaufmann.
- Leclerc, G., Ilyas, A., Engstrom, L., Park, S. M., Salman, H., and Madry, A. FFCV: Accelerating training by removing data bottlenecks. In *Computer Vision and Pattern Recognition (CVPR)*, 2023. <https://github.com/libffcv/ffcv/>. commit 6c3be0cabf1485aa2b6945769dbd1c2d12e8faa7.
- Loshchilov, I. and Hutter, F. Sgdr: Stochastic gradient descent with warm restarts. *arXiv: Learning*, 2016. URL <https://api.semanticscholar.org/CorpusID:14337532>.
- Loshchilov, I. and Hutter, F. Decoupled weight decay regularization. In *International Conference on Learning Representations*, 2017. URL <https://api.semanticscholar.org/CorpusID:53592270>.
- Ma, J., Bai, S., and Zhou, C. Pretrained diffusion models for unified human motion synthesis. *ArXiv*, abs/2212.02837, 2022. URL <https://api.semanticscholar.org/CorpusID:254274884>.

- Maji, S., Rahtu, E., Kannala, J., Blaschko, M. B., and Vedaldi, A. Fine-grained visual classification of aircraft. *ArXiv*, abs/1306.5151, 2013. URL <https://api.semanticscholar.org/CorpusID:2118703>.
- Meng, Y., Huang, J., Zhang, Y., and Han, J. Generating training data with language models: Towards zero-shot language understanding. *ArXiv*, abs/2202.04538, 2022. URL <https://api.semanticscholar.org/CorpusID:246680398>.
- Mimura, M., Ueno, S., Inaguma, H., Sakai, S., and Kawahara, T. Leveraging sequence-to-sequence speech synthesis for enhancing acoustic-to-word speech recognition. *2018 IEEE Spoken Language Technology Workshop (SLT)*, pp. 477–484, 2018. URL <https://api.semanticscholar.org/CorpusID:61806902>.
- Misra, I. and Maaten, L. v. d. Self-supervised learning of pretext-invariant representations. In *Proceedings of the IEEE/CVF conference on computer vision and pattern recognition*, pp. 6707–6717, 2020.
- Nilsback, M.-E. and Zisserman, A. Automated flower classification over a large number of classes. *2008 Sixth Indian Conference on Computer Vision, Graphics & Image Processing*, pp. 722–729, 2008. URL <https://api.semanticscholar.org/CorpusID:15193013>.
- Oord, A. v. d., Li, Y., and Vinyals, O. Representation learning with contrastive predictive coding. *arXiv preprint arXiv:1807.03748*, 2018.
- Radford, A., Kim, J. W., Hallacy, C., Ramesh, A., Goh, G., Agarwal, S., Sastry, G., Askell, A., Mishkin, P., Clark, J., Krueger, G., and Sutskever, I. Learning transferable visual models from natural language supervision. In *International Conference on Machine Learning*, 2021. URL <https://api.semanticscholar.org/CorpusID:231591445>.
- Ramesh, A., Pavlov, M., Goh, G., Gray, S., Voss, C., Radford, A., Chen, M., and Sutskever, I. Zero-shot text-to-image generation. *ArXiv*, abs/2102.12092, 2021. URL <https://api.semanticscholar.org/CorpusID:232035663>.
- Recht, B., Roelofs, R., Schmidt, L., and Shankar, V. Do imagenet classifiers generalize to imagenet? In *International Conference on Machine Learning*, 2019. URL <https://api.semanticscholar.org/CorpusID:67855879>.
- Rewatbowornwong, P., Tritrong, N., and Suwajanakorn, S. Repurposing gans for one-shot semantic part segmentation. *IEEE Transactions on Pattern Analysis and Machine Intelligence*, 45:5114–5125, 2021. URL <https://api.semanticscholar.org/CorpusID:232147296>.
- Rombach, R., Blattmann, A., Lorenz, D., Esser, P., and Ommer, B. High-resolution image synthesis with latent diffusion models. *2022 IEEE/CVF Conference on Computer Vision and Pattern Recognition (CVPR)*, pp. 10674–10685, 2021. URL <https://api.semanticscholar.org/CorpusID:245335280>.
- Saharia, C., Ho, J., Chan, W., Salimans, T., Fleet, D. J., and Norouzi, M. Image super-resolution via iterative refinement. *IEEE Transactions on Pattern Analysis and Machine Intelligence*, 45:4713–4726, 2021. URL <https://api.semanticscholar.org/CorpusID:233241040>.
- Saharia, C., Chan, W., Saxena, S., Li, L., Whang, J., Denton, E. L., Ghasemipour, S. K. S., Ayan, B. K., Mahdavi, S. S., Lopes, R. G., Salimans, T., Ho, J., Fleet, D. J., and Norouzi, M. Photorealistic text-to-image diffusion models with deep language understanding. *ArXiv*, abs/2205.11487, 2022. URL <https://api.semanticscholar.org/CorpusID:248986576>.
- Sariyildiz, M. B., Karteek, A., Larlus, D., and Kalantidis, Y. Fake it till you make it: Learning transferable representations from synthetic imagenet clones. *2023 IEEE/CVF Conference on Computer Vision and Pattern Recognition (CVPR)*, pp. 8011–8021, 2022. URL <https://api.semanticscholar.org/CorpusID:257772061>.
- Silver, D., Schrittwieser, J., Simonyan, K., Antonoglou, I., Huang, A., Guez, A., Hubert, T., baker, L., Lai, M., Bolton, A., Chen, Y., Lillicrap, T. P., Hui, F., Sifre, L., van den Driessche, G., Graepel, T., and Hassabis, D. Mastering the game of go without human knowledge. *Nature*, 550:354–359, 2017. URL <https://api.semanticscholar.org/CorpusID:205261034>.
- Sun, D., Vlasic, D., Herrmann, C., Jampani, V., Krainin, M., Chang, H., Zabih, R., Freeman, W. T., and Liu, C. Autoflow: Learning a better training set for optical flow. *2021 IEEE/CVF Conference on Computer Vision and Pattern Recognition (CVPR)*, pp. 10088–10097, 2021. URL <https://api.semanticscholar.org/CorpusID:233443829>.
- Tian, Y., Krishnan, D., and Isola, P. Contrastive multiview coding. In *European Conference on Computer Vision*, 2019. URL <https://api.semanticscholar.org/CorpusID:189762205>.
- Tian, Y., Fan, L., Isola, P., Chang, H., and Krishnan, D. Stablerep: Synthetic images from text-to-image

- models make strong visual representation learners. *ArXiv*, abs/2306.00984, 2023. URL <https://api.semanticscholar.org/CorpusID:258999759>.
- Tomasev, N., Bica, I., McWilliams, B., Buesing, L. H., Pascanu, R., Blundell, C., and Mitrovic, J. Pushing the limits of self-supervised resnets: Can we outperform supervised learning without labels on imagenet? In *First Workshop on Pre-training: Perspectives, Pitfalls, and Paths Forward at ICML 2022*, 2022. URL <https://openreview.net/forum?id=oNIKfCtr8wH>.
- Tremblay, J., Prakash, A., Acuna, D., Brophy, M., Jampani, V., Anil, C., To, T., Cameracci, E., Boochoon, S., and Birchfield, S. Training deep networks with synthetic data: Bridging the reality gap by domain randomization. In *Proceedings of the IEEE conference on computer vision and pattern recognition workshops*, pp. 969–977, 2018.
- Vanherle, B., Moonen, S., Van Reeth, F., and Michiels, N. Analysis of training object detection models with synthetic data. *arXiv preprint arXiv:2211.16066*, 2022.
- Wang, H., Ge, S., Xing, E. P., and Lipton, Z. C. Learning robust global representations by penalizing local predictive power. In *Neural Information Processing Systems*, 2019. URL <https://api.semanticscholar.org/CorpusID:173188134>.
- Wang, Z., Pang, T., Du, C., Lin, M., Liu, W., and Yan, S. Better diffusion models further improve adversarial training. *ArXiv*, abs/2302.04638, 2023. URL <https://api.semanticscholar.org/CorpusID:256697167>.
- whan Kim, Y., Jin, S., Panda, R., Kuehne, H., Karlinsky, L., Mishra, S., Saligrama, V., Saenko, K., Oliva, A., and Feris, R. S. How transferable are video representations based on synthetic data? In *Neural Information Processing Systems*, 2022. URL <https://api.semanticscholar.org/CorpusID:252671690>.
- Wu, Z., Xiong, Y., Yu, S. X., and Lin, D. Unsupervised feature learning via non-parametric instance discrimination. In *Proceedings of the IEEE conference on computer vision and pattern recognition*, pp. 3733–3742, 2018.
- Ye, M., Zhang, X., Yuen, P. C., and Chang, S.-F. Unsupervised embedding learning via invariant and spreading instance feature. In *Proceedings of the IEEE/CVF conference on computer vision and pattern recognition*, pp. 6210–6219, 2019.
- You, Y., Gitman, I., and Ginsburg, B. Large batch training of convolutional networks. *arXiv: Computer Vision and Pattern Recognition*, 2017. URL <https://api.semanticscholar.org/CorpusID:46294020>.
- Zbontar, J., Jing, L., Misra, I., LeCun, Y., and Deny, S. Barlow twins: Self-supervised learning via redundancy reduction. In *International Conference on Machine Learning*, pp. 12310–12320. PMLR, 2021.

## A. Overview

This supplementary document enhances the primary paper in the following ways:

1. Provides additional insights into the methodology (complements **Section 3**).
2. Offers further details on training configurations, model setups, and the image generation procedure (complements **Section 4**).

## B. Background: Joint-embedding SSL

One of the most successful self-supervised learning paradigms is joint-embedding SSL. Joint-Embedding Self-Supervised Learning (SSL) operates on the concept of instance-based views, where each image is treated as a distinct class (Dosovitskiy et al., 2014; Assran et al., 2023). This methodology capitalizes on data augmentation to generate diverse views of the same image. A notable subset of this approach is contrastive SSL techniques (Oord et al., 2018; He et al., 2020; Chen et al., 2020), which, within joint-embedding frameworks, aim to closely align the output embeddings of an image with those of its augmented version. Concurrently, these techniques strive to differentiate these embeddings from those of other images and their respective augmentations. Such methods are commonly implemented in Siamese network architectures (Chen & He, 2021), characterized by two parallel branches that are identical in structure and share the same weights. In our research, we focus on two joint-embedding frameworks: SimCLR (Chen et al., 2020) and BarlowTwins (Zbontar et al., 2021).

### B.1. Training and evaluating Joint-embedding SSL

Given an unlabelled dataset  $D = \{x_1, x_2, \dots, x_n\}$  where  $x_i \in X \subset R^d$ , represents the  $i^{th}$  input. Any SSL method involves designing a pretext-task  $S$  which utilizes pseudo-labels/feature representations  $v_i \in Y$ . We train a model  $f(x)$  on  $D_{train} \subset D$  such that  $P(v|x)$ , i.e. the conditional distribution of pseudo-labels given the input satisfies the pre-text task  $S$ . Eventually, we freeze the learned model parameters and train linear classifiers  $g(f(x))$  on top of the model. The linear classifier is trained in a supervised manner via empirical risk minimization,  $L(g(f(x)), y)$ , where  $y$  is the ground truth labels and  $L$  is the training objective.

## C. Method

### C.1. Mixing in Distillation SSL

Recent methods such as DINO (Caron et al., 2021), exploit architectural tricks inspired by knowledge distillation (KD) (Hinton et al., 2015). The KD technique involves training a ‘student’ network to emulate the output representations of a ‘teacher’ network. The teacher network’s weights are dynamically updated as a running average of the student network’s weights or are shared with the student network (Grill et al., 2020). Notably, in this configuration, gradients are not backpropagated through the teacher network (Chen & He, 2021).

**DINO and DINO + DiffMix:** The original implementation of DINO (Caron et al., 2021) employs a multi-crop strategy to process multiple scaled views of an image. Specifically, for a given image, a set  $V$  of different views is generated, comprising two global views ( $x_1^g$  and  $x_2^g$ ) at higher resolutions and multiple local views ( $x_k^l$  for  $k$  ranging from 1 to 8) at lower resolutions. Consider the training framework for DINO leverages the following KD framework: a student network  $g_{\theta_s}$ , parameterized by  $\theta_s$ , is trained to align with the output of a teacher network  $g_{\theta_t}$ , parameterized by  $\theta_t$ . All views (local + global) are processed by the student, while only the global views are handled by the teacher, promoting a ‘local-to-global’ learning correspondence.

Building on this foundation, we introduce image mixing in DINO, termed DINO + DiffMix. In this modified approach, instead of using two global views and eight local views from each real image, we employ a mix of real and synthetic images. Specifically, we use one global view and six local views from a real image, supplemented by one global view and two local views from a corresponding synthetic image as shown in Figure 2 (C). This particular mix of real and synthetic views was determined empirically, and we explore varying levels of mixing and its impact on DINO model performance in Section 5.3. Consequently, our modified set includes a global view from a real image ( $x_1^g$ ), a global view from a synthetic image ( $\hat{x}_2^g$ ), and four local views each from the real ( $x_k^l \forall k \in [1, 4]$ ) and synthetic ( $\hat{x}_k^l \forall k \in [1, 4]$ ) images. In this framework, both the student and teacher networks generate probability distributions over  $K$  dimensions, denoted as  $P_s$  and  $P_t$ , respectively. These probabilities are derived by normalizing the networks’ outputs using a softmax function. Specifically,

$$P_s(X)^{(i)} = \frac{\exp(g_{\theta_s}(X)^{(i)}/\tau_s)}{\sum_{k=1}^K \exp(g_{\theta_s}(X)^{(k)}/\tau_s)}$$

The parameter  $\tau_s$ , a positive temperature value, modulates the sharpness of the student network’s output distribution. The set  $X_s$  for the student encompasses all views, namely  $\{x_1^g, \tilde{x}_2^g, x_k^l, \tilde{x}_k^l\} \forall k \in [1,4]$ , named as a set  $\tilde{V}$ . In a parallel manner, the teacher network’s output distribution is influenced by its own temperature parameter  $\tau_t$ . However, the set  $X_t$  for the teacher is restricted to only global views  $\{x_1^g, \tilde{x}_2^g\}$ .

## D. Experiments

### D.1. Training configurations

Our training employs FFCV-SSL (Bordes et al., 2023), an extended version of the FFCV library (Leclerc et al., 2023) with added support for SSL data augmentations, enhancing training speed and feasibility within our limited resources. We have adapted the code for the DINO framework, in addition to Barlow Twins and SimCLR models. For these models, the LARS (You et al., 2017) optimizer with a learning rate of 1 is used, while DINO models utilize the AdamW (Loshchilov & Hutter, 2017) optimizer with a learning rate of 0.0005. All experiments are conducted with a consistent batch size of 256, employing the Cosine Decay scheduler (Loshchilov & Hutter, 2016). Offline linear probes are conducted with the AdamW optimizer at a learning rate of 0.0001 across all experiments, utilizing only real images for training in every case.

### D.2. Model configurations

In our experiments, SimCLR and Barlow Twins utilize ResNet-50 as the base encoder, while DINO employs Vision Transformer Small/16 (ViT-S/16) as its backbone. Additionally, a linear layer mapping the representation size to the class count is added atop the encoder. The representation size for SimCLR and Barlow Twins is 2048, whereas for DINO, it’s set to 65536, identified as optimal for DINO (Caron et al., 2021).

### D.3. Generating images

Our process for generating images utilizes 50 diffusion steps, as noted in (Sariyildiz et al., 2022), expanding the step count beyond 50 appears to be unnecessary. For the IN-100 dataset, we use various guidance scales (2,3,6,8,12) to generate images. Following the findings of (Azizi et al., 2023), we produce large images with a resolution of  $512 \times 512$  pixels, batched in groups of 64. For the IN-1K dataset, a consistent guidance scale of 8 is applied. We set the random seed to 25 for reproducibility. By generating images before training, we reduce the overall training time.